

ANALYZING NMR SPECTRA WITH THE MORLET WAVELET

Aimamorn Suvichakorn and Jean-Pierre Antoine

Institut de physique théorique (FYMA)
Université catholique de Louvain
B-1348 - Louvain-la-Neuve, Belgium
email: jean-pierre.antoine@uclouvain.be

ABSTRACT

We study the time-scale representation provided by the Morlet wavelet transform for characterizing NMR signals. From an analytical analysis and simulations, we conclude that the wavelet shows a satisfactory performance even when a baseline, an additive Gaussian noise or a solvent are present in the signals. It can also cope with non-Lorentzian lineshapes which commonly occur because of the inhomogeneous distribution of molecules in a substance. These results mean that the Morlet wavelet transform is a potential tool to quantify in vivo NMR signals.

1. INTRODUCTION

A nuclear magnetic resonance (NMR) signal is acquired when the nuclei in a substance are excited by a radio frequency pulse, and re-radiated. This results in an exponential decaying sine wave, which has a so-called Lorentzian lineshape in the frequency domain. The frequency of the peak of the signal depends upon the nucleus and is therefore typical to each substance. The amplitude in the time domain, i.e. the area in the frequency domain, depends on the amount of those nuclei, which can then relate to the concentration of the substance [1]. Therefore, a good quantification technique is essential for the interpretation of the NMR signals.

For this purpose, a number of techniques have been proposed, to be used both in time or in frequency domains (see [2, 3]). There also exists the wavelet transform, which yields a time-scale representation. Analyzing in the two domains simultaneously makes it more efficient than the Fourier transform, which gives only spectral information. In addition, a small perturbation of a signal which may occur during the data acquisition will result only in a small, local modification of the wavelet transform.

Among several types of wavelet transforms, the continuous wavelet transform technique [4, 5] can estimate the frequency and amplitude of the spectral line directly from phase and modulus of the wavelet transform and no linear model is needed as in the techniques based on the discrete wavelet transform [6]. The present paper will exploit that property of the continuous wavelet transform, with the Morlet wavelet in particular, and focus on problems such as the baseline, the solvent and non-Lorentzian lineshapes, which commonly appear in NMR spectroscopy.

2. METHODOLOGY

In order to characterize a signal, the wavelet-based techniques first detect the frequencies in NMR signals and then estimate the amplitude at each detected frequency.

The wavelet transform of a signal $s(t)$ with respect to a mother wavelet $g(t)$ is

$$S(\tau, a) = \frac{1}{2\pi} \sqrt{a} \int S(\omega) G^*(a\omega) e^{i\omega\tau} d\omega, \quad (1)$$

where $S(\omega)$ is the Fourier transform of the signal, $a > 0$ is a dilation parameter, $\tau \in \Re$ is a translation parameter and $G^*(\omega)$ is the complex conjugate of the Fourier transform of $g(t)$. Given a Lorentzian signal $s(t)$, namely

$$\begin{aligned} s(t) &= Ae^{-Dt} e^{i(\omega_s t + \phi)} \\ S(\omega) &= 2\pi A e^{i\phi} \delta(\omega - (\omega_s + Di)), \end{aligned} \quad (2)$$

where D and ϕ are the damping factor and the phase of the signal, the Morlet wavelet transform of $s(t)$ is

$$\begin{aligned} S(\tau, a) &= \sqrt{a} A e^{i\phi} e^{-D\tau} e^{i\omega_s \tau} G_M^*(a(\omega_s + Di)) \\ &= s(\tau) G_M^*(a(\omega_s + Di)), \end{aligned} \quad (3)$$

where

$$\begin{aligned} g_M(t) &= \frac{1}{2\pi\sigma} e^{-\frac{1}{2\sigma^2} t^2} e^{i\omega_0 t} + \varepsilon(t) \\ G_M(\omega) &= e^{-\frac{\sigma^2}{2} (\omega - \omega_0)^2} + \varepsilon^*(\omega), \end{aligned} \quad (4)$$

is the Morlet wavelet whose frequency and width are denoted by ω_0 and σ . The correction term ε is negligible when $\sigma\omega_0 \geq 5.5$, and will be omitted henceforth. It can be seen that the modulus of $S(\tau, a)$ is maximum, i.e. $\frac{\partial}{\partial a} S(\tau, a) \rightarrow 0$, when $\frac{\partial}{\partial a} G \rightarrow 0$. Since $a \in \Re$ and with the assumption that $\omega_s \gg D$, the maximum can be found at the scale $a_r = \omega_0/\omega_s$, which then gives

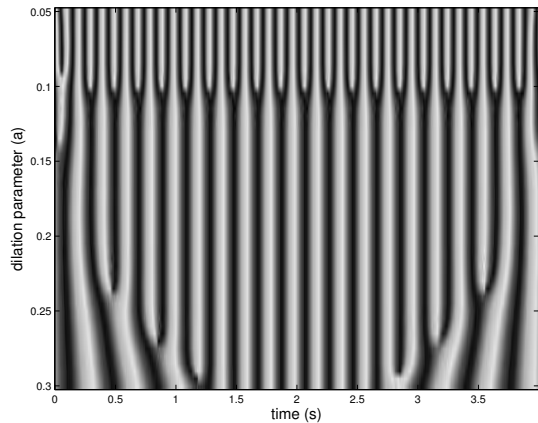
$$G^*(a_r(\omega_s + Di)) = \exp\left(\frac{\sigma a_r D}{\sqrt{2}}\right)^2, \quad (5)$$

and consequently

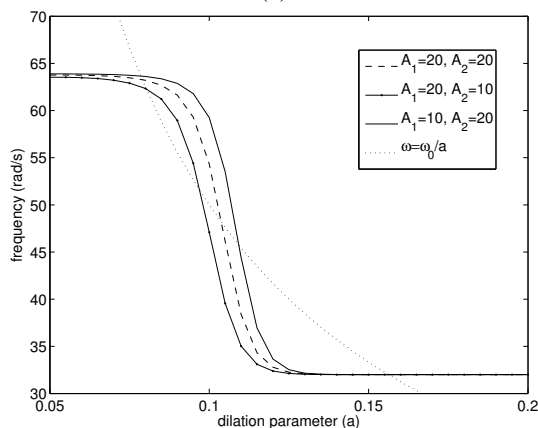
$$S_{a_r}(\tau) = \sqrt{a_r} \exp\left(\frac{\sigma a_r D}{\sqrt{2}}\right)^2 s(\tau), \quad (6)$$

is also identical to the signal $s(t)$ scaled by a coefficient depending on a still-unknown D . Next, consider the phase of the Morlet wavelet transform along the scale a_r ,

$$\begin{aligned} \angle S_{a_r}(\tau) &= \omega_s \tau + \phi \\ \omega_s &= \frac{\partial}{\partial \tau} \angle S_{a_r}(\tau). \end{aligned} \quad (7)$$



(a)



(b)

Figure 1: (a) Phase of the wavelet transform of $g(t)$ with $\omega_s = 32$ and 64 rad/s and (b) its instantaneous frequencies. Note: $\sigma = 1$, $\omega_0 = 5$, $F_s = 256$, $l = 1024$.

That is, the instantaneous frequency on the scale a_r of the Morlet transform is ω_s . By Eq. (7), the phase ϕ can also be recovered, if needed. This method is also applicable to an n -frequency signal if its frequencies are *sufficiently* far away from each other that $G^*(a\omega)$ can treat each spectral line independently [7]. As illustrated in Fig. 1 (b), the instantaneous frequency of the wavelet transform of a signal with $\omega_s = 32$ and 64 rad/s converges to the two frequencies of the signal at the scale $\omega_0/32$ and $\omega_0/64$. It can also be seen that Eq. (7) works not only on the scale $a_r = \omega_0/\omega_s$ but also for a wide range of a . Whenever two frequencies are very close to each other (this also depends on the sampling frequency and the relative amplitudes of both frequencies), increasing the frequency of the Morlet function ω_0 can better localize and distinguish the overlapping frequencies. However, ω_0 should not be too high that the transform becomes noisy and unreliable.

Next, consider the modulus of the wavelet transform along a_r ,

$$|S_{a_r}(\tau)| = \sqrt{a_r} \exp\left(\frac{\sigma a_r D}{\sqrt{2}}\right)^2 |s(\tau)|$$

$$\ln |S_{a_r}(\tau)| = \frac{1}{2} \ln a + \left(\frac{\sigma a_r D}{\sqrt{2}}\right)^2 + \ln A - D\tau.$$

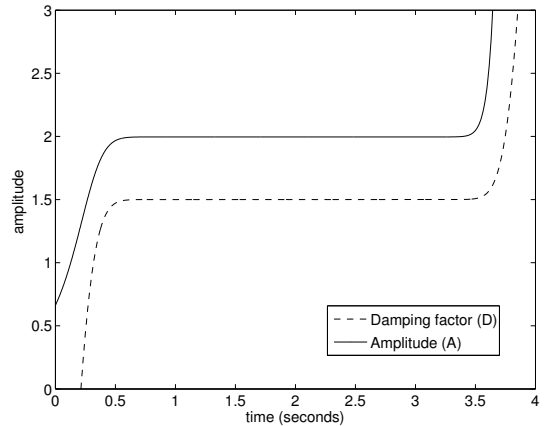


Figure 2: Derived damping factor and amplitude of a signal with $D=1.5$, $A=2$, and $\omega_s = 32$ rad/s, at a_r . Same parameters as in Fig. 1.

That is,

$$D = -\frac{\partial}{\partial \tau} \ln |S_{a_r}(\tau)|. \quad (8)$$

Knowing D can now lead to the estimation of the amplitude resonance A of the signal, i.e.

$$A = |s(t)| e^{D\tau}. \quad (9)$$

The Morlet wavelet is the most frequently used in practical because of its simple numerical implementation and the vanishing of the third-order differentiation of its phase can also simplify the computation [5]. In addition, there is no need to compute the wavelet transform at all scales. A rough approximation of the scale a_r may be read from the Fourier transform of the signal, or derived from *a priori* knowledge. Then, a more precise value of a_r can be calculated iteratively using the ridge extraction in [5]. If the signal also includes noise, the authors of [4] suggested averaging the instantaneous frequency, i.e.

$$\bar{\Omega}_a = \frac{1}{T} \int_{\tau_0}^{\tau_0+T} \Omega_a(\tau) d\tau,$$

where $\Omega_a(\tau) = \frac{\partial}{\partial \tau} \angle S_{a_r}(\tau)$. Fig. 3 shows that the averaging gives a more stable $\bar{\Omega}$ as it creates a wider range of steady points along a . Note that Eq. (6) differs from the literature which approximates the wavelet transform by the Taylor series and omits the term D .

2.1 Apodization

In general, using the Fourier transform to analyze a signal can produce erroneous results due to the discrete implementation, e.g. aliasing, picket-fence effect, etc. Basically, this means that the sampling frequency (F_s) and the length of the signal (l) need to be carefully selected. The problem becomes more severe when two frequencies are close together. To solve this, the frequency resolution can be increased by zero padding the signal. However, this may introduce a ringing effect, which is another consequence of a finite data set. Techniques such as decay padding, data-tapering window

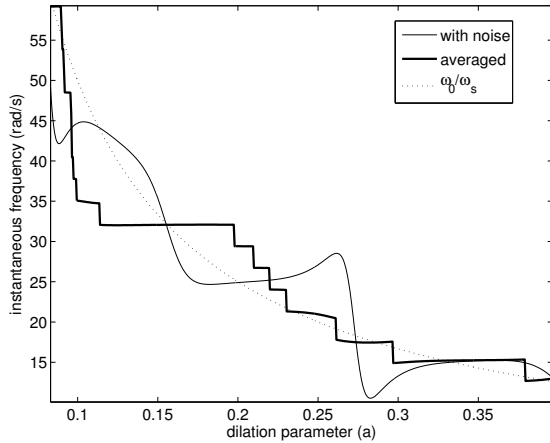


Figure 3: The instantaneous frequency of a signal of 32 rad/s with SNR=10 (additive complex Gaussian noise with $\sigma_n = 0.079$) derived by the Morlet wavelet at $t = 4.7$ s. Note: $\sigma=1$, $\omega_0=5$, $F_s=800$, $l=1024$.

or wrap-around can be applied to reduce this boundary effect [8]. In NMR spectroscopy, the Gaussian or Lorentzian window is commonly used and such windowing process is known as *apodization*. For the continuous wavelet transform, the boundary effect increases linearly with a , which can be seen as a cone in Fig. 1 (a) and Fig. 2. However, by using Ω outside this cone, there is no need to apply a tapering window to the signal.

2.2 Baseline

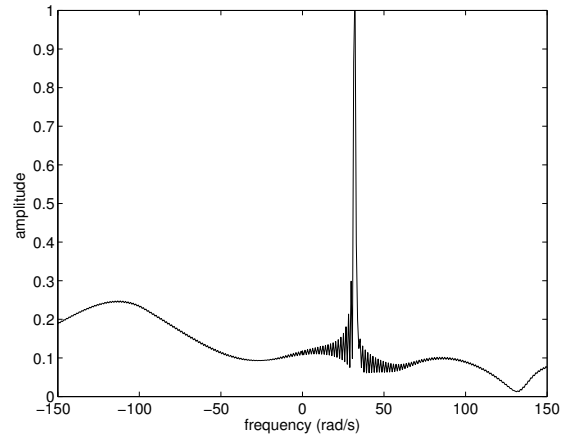
The baseline corresponds to underlying broad resonances of large molecules, known as macromolecules, and lipids. It can affect the characterization of an NMR signal when the Fourier transform is used. Here, the baseline is modelled by cubic splines to study the performance of the wavelet transform. Fig. 4 shows that the baseline has no effect with the derived frequency or amplitude. In fact, the baseline has its effect only at the left edge of the transform. Although splines are used to simplify the problem, if the real baseline satisfies the assumption that it converges much faster than the actual signals, using the wavelet transform to derive the frequency and amplitude of an NMR signal should still work without removing the baseline beforehand.

2.3 Solvent

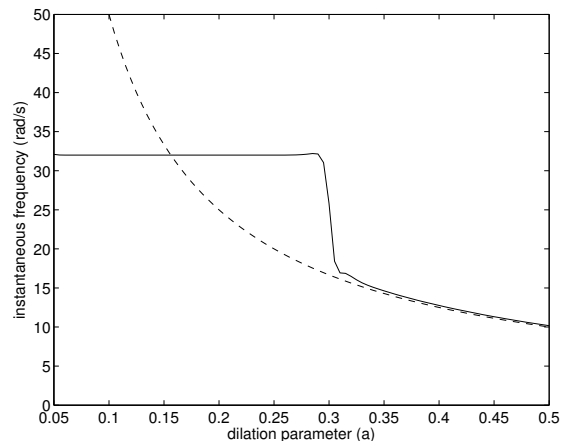
The Morlet wavelet transform sees the signal at each frequency individually, therefore it can work well even if the amplitude at various frequencies are hugely different, which normally occurs when there is a peak of solvent in the signal. As an example, the Morlet wavelet transform has been applied to a signal

$$s(t) = 100e^{-8.5t}e^{i32t} + e^{-1.5t}e^{i60t} + e^{-0.5t}e^{i90t} + e^{-t}e^{i120t} + e^{-2t}e^{i150t},$$

as seen in Fig. 5. It is a signal with an amplitude of 100 at 32 rad/s and 1 elsewhere. The high amplitude can affect other frequencies if they are close to each other. Using the aforementioned method, the amplitude of 1 can be extracted



(a)



(b)

Figure 4: (a) The Fourier transform of a 32-rad/s signal with baseline. Its instantaneous frequency is in (b), compared to the dotted line of ω_0/a . Parameters used are the same as in Fig. 1. The baseline is modelled by a cubic spline.

as 0.98, 0.91, 0.99 and 0.97 respectively. The error ranges within 1.2-8.9%, without any preprocessing.

3. NON-LORENTZIAN LINESHAPE

The Lorentzian lineshape assumes that the homogeneous lifetime broadening and pure dephasing are equally contributed from each individual molecule. However, molecules have different relaxation rates in general. In addition, there are other sources, such as the inhomogeneous distribution of the molecules, Doppler shifts or site differences of molecules in the solution, that can cause the inhomogeneous broadening. These effects are typically modelled by a Gaussian lineshape [9]. Since the inhomogeneous broadening is often significantly larger than the lifetime broadening, the Gaussian lineshape is often dominant.

3.1 Gaussian and Voigt lineshapes

Let us define a pure Gaussian function with a frequency at ω_s as

$$s_G(t) = Ae^{-\gamma^2 t^2} e^{i\omega_s t}, \quad (10)$$

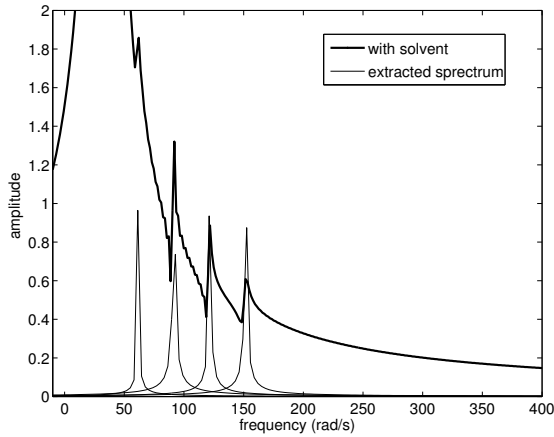


Figure 5: The Fourier transform of a signal with different amplitudes and the spectrum extracted by the Morlet wavelet.

where γ is a Gaussian damping factor. By solving the Gaussian integral, its Morlet wavelet transform at the scale $a_r = \omega_0/\omega_s$ is then

$$S_{G,a_r}(\tau) = k_1 A e^{-k_2 \tau^2} e^{i\omega_s \tau}, \quad (11)$$

where

$$k_1 = \sqrt{\frac{a_r}{2\pi(2\gamma\sigma^2 a_r^2 + 1)}}$$

$$k_2 = \frac{\gamma}{2\gamma\sigma^2 a_r^2 + 1},$$

which is also a Gaussian function at the frequency ω_s . This new Gaussian function has its instantaneous frequency equal to ω_s . Therefore, as in the processing of the Lorentzian lineshape, A and γ can be obtained as follows:

1. Find $\omega_s = \frac{\partial}{\partial \tau} \angle S_{G,a_r}(\tau)$.
2. Find γ from $\frac{\partial^2}{\partial \tau^2} \ln |S_{G,a_r}(\tau)|$.
3. Find A from the calculated ω_s and γ .

Note that the scale $a_r = \omega_0/\omega_s$ does not give exactly the maximum modulus of the wavelet transform, but it is acceptable on the condition that $a \in \mathfrak{R}$ and $\omega_s \gg D$.

On the other hand, if the lineshape is intermediate between a Gaussian and a Lorentzian form, the spectrum can be fitted to a convolution of the two functions. Such lineshape is known as a Voigt profile. It can be used to resolve the lineshape into homogeneous (Lorentzian) and inhomogeneous (Gaussian) components. The Morlet wavelet transform at the scale $a_r = \omega_0/\omega_s$ of a Voigt lineshape

$$s_V(t) = A e^{-\gamma t^2} e^{-Dt} e^{i\omega_s t}, \quad (12)$$

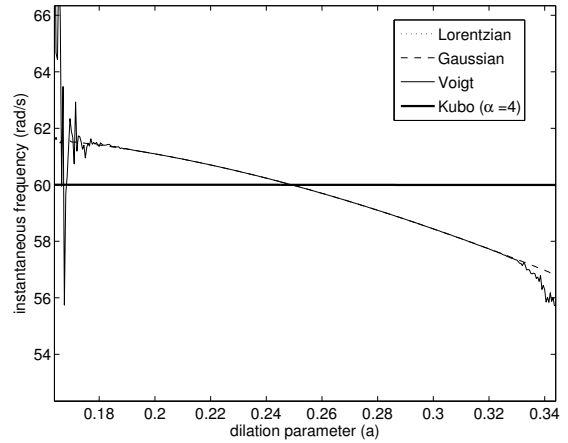
is

$$S_{V,a_r}(\tau) = k_3 A e^{-k_2(\tau+k_4)^2} e^{i\omega_s \tau}, \quad (13)$$

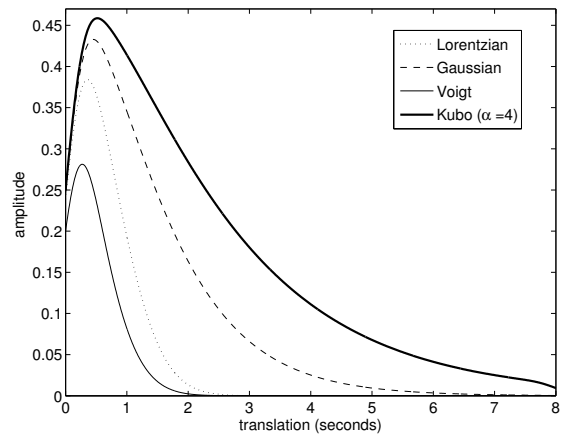
where

$$k_3 = k_1 e^{\frac{D^2}{4\gamma}}$$

$$k_4 = \frac{D}{2\gamma}.$$



(a)



(b)

Figure 6: (a) The comparison of the instantaneous frequency of the Morlet wavelet transform of a signal of a frequency 60 rad/s with different lineshapes, e.g. Lorentzian $s(t) = e^{-t} e^{i60t}$, Gaussian $s(t) = e^{-t^2} e^{i60t}$, Voigt $s(t) = e^{-t} e^{-t^2} e^{i60t}$ and Kubo $s(t) = e^{-0.25(e^{-t}-1+t)} e^{i60t}$ at $t = 4.7$ s. The modulus of the Morlet wavelet transform of each line at $a_r = \omega_0/60$ is in (b). Note: $\sigma=1$, $\omega_0=15$, $F_s=800$, $l=1024$.

That is, at the scale a_r , the Morlet wavelet transform of the Voigt lineshape is also a Gaussian function with the same width as that of the Gaussian lineshape, but shifted in time and amplitude modified. Its instantaneous frequency is also equal to ω_s along the scale a_r , as shown in Fig. 6 (a). In addition, the second derivative of the modulus of the wavelet transform can be used to describe the second-order broadening of the lineshape, i.e. γ , be it Gaussian or Voigt, by

$$\gamma = -\frac{0.5}{\left(\frac{\partial^2}{\partial \tau^2} \ln |S_{G,a_r}(\tau)|\right)^{-1} + \sigma^2 a_r^2}. \quad (14)$$

This is confirmed by the convergence to the same value for both lineshapes in Fig. 7 (a).

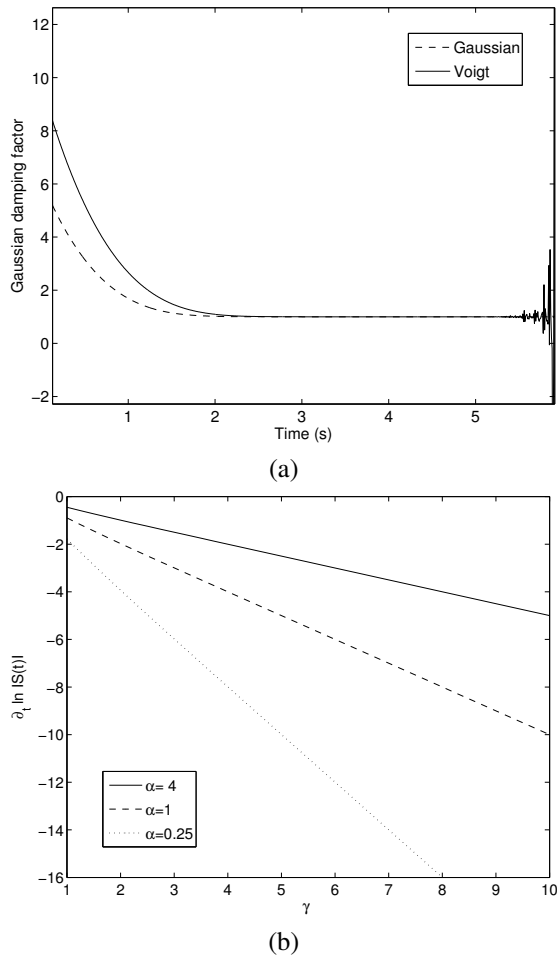


Figure 7: (a) The Gaussian damping factor derived from Eq. (14) and (b) $\frac{\partial}{\partial \tau} \ln |S_{G,a_r}(\tau)|$ with respect to Kubo's γ .

3.2 Kubo's lineshape

The interaction between homogeneous and inhomogeneous broadenings of the lineshape depends on the time scale. For example, if the relaxation time (T_2) is much longer than any effects modulating the energy of a molecule, the lineshape will approach the homogeneous lineshape. On the contrary, if T_2 is short, the lineshape is likely to be Gaussian. In [10], a so-called Gaussian-Markovian modulation, namely

$$s_K(t) = A e^{-\frac{\zeta^2}{\gamma^2}(e^{-\gamma t} - 1 + \gamma t)} e^{i\omega_s t}, \quad (15)$$

is used to account for this time scale. The parameter γ is inversely proportional to T_2 and ζ is the amplitude of the solvent-induced fluctuations in the frequency. If $\alpha = \gamma/\zeta \ll 1$, the lineshape becomes Gaussian, whereas $\alpha \gg 1$ leads to Lorentzian. Solving Eq. (15) seems to be complicated, though may be possible. However, the Morlet's instantaneous frequency at the scale $a_r = \omega_0/\omega_s$ is still capable of deriving the ω_s , even better than the Gaussian lineshape, as shown in Fig. 6 (a). The damping parameters can also be derived by a linear relation with $\frac{\partial}{\partial \tau} \ln |S_{G,a_r}(\tau)|$, as seen in Fig. 7 (b), whereas α relates directly to $\frac{\partial^2}{\partial \tau^2} \ln |S_{G,a_r}(\tau)|$.

4. CONCLUSION

This paper presents an analytical analysis of the Morlet wavelet transform to quantify NMR signals. The wavelet works well with Lorentzian, Gaussian, Voigt and Kubo line-shapes. It is also efficient when baseline, noise or solvent are present in the signal. The method works well with a signal whose frequencies are sufficiently far from each other. Increasing the frequency of the Morlet wavelet can also help resolving the frequency components that are close to each other. However, for use in *in vivo* signals which will be acquired by our partners at UCBL (Lyon) and EPFL (Lausanne), the method needs further development to cope with severely overlapping frequencies.

Acknowledgment. The work is parts of the Advanced Signal Processing for Ultra-fast Magnetic Resonance (FAST) project funded by the Marie-Curie Research Network, (MRTN-CT-2006-035801), <http://www.fast-mariecurie-rtn-project.eu>. The authors would also like to thank Prof. D. Graveron-Demilly, H. Ratiney and S. Cavassila, our partners at UCBL for their invaluable advice, and V. Mlynarik and C. Cudalbu (EPFL) for their collaboration.

REFERENCES

- [1] J.P. Hornak. *The Basics of NMR*. <http://www.cis.rit.edu/htbooks/nmr/>. 1997.
- [2] L. Vanhamme, T. Sundin, P. Van Hecke, and S. Van Huffel. MR spectroscopic quantitation: A review of time domain methods. *NMR in Biomedicine*, 14(4):233–46, 2001.
- [3] S. Mierisová and M. Ala-Korpela. MR spectroscopy quantitation: a review of frequency domain methods. *NMR in Biomedicine*, 14(4):247–59, 2001.
- [4] P. Guillemain, R. Kronland-Martinet, and B. Martens. Estimation of spectral lines with the help of the wavelet transform, applications in NMR spectroscopy. In Y. Meyer, editor, *Wavelets and applications (Proc. Marseille 1989)*, pages 38–60. Springer, Berlin, and Masson, Paris, 1991.
- [5] N. Delprat, B. Escudié, P. Guillemain, R. Kronland-Martinet, P. Tchamitchian, and B. Torrèsani. Asymptotic wavelet and Gabor analysis extraction of instantaneous frequencies. *IEEE Transactions on Information Theory*, 38(2):644–664, March 1992.
- [6] F. Dancea and U. Günther. Automated protein NMR structure determination using wavelet de-noised NOESY spectra. *Journal of Biomolecular NMR*, 33(3):139–152, 2005.
- [7] D. Barache, J-P. Antoine, and J-M. Dereppe. The continuous wavelet transform, an analysis tool for NMR spectroscopy. *Journal of Magnetic Resonance*, 128:1–11, 1997.
- [8] P. Addison. *The Illustrated Wavelet Transform Handbook*. Institute of Physics Publishing, London, 2002.
- [9] S. Franzen. Lecture notes on molecular spectroscopy. Department of Chemistry, NC State University, 2002. <http://chsfpc5.chem.ncsu.edu/~franzen/CH795Z/>.
- [10] R. Kubo. *Advances in Chemical Physics: Stochastic Processes in Chemical Physics*, vol. 15, A Stochastic Theory of Line Shape, 101–127. 1969.